https://doi.org/10.5194/egusphere-2026-3648
Preprint. Discussion started: 30 June 2026

How to diagnose barotropic Rossby wave resonance along a circumglobal jetstream?

Volkmar Wirth[1], Tobias Hempel[1], and Nili Harnik[2]

[1]Institute for Atmospheric Physics, Johannes Gutenberg University Mainz, Becherweg 21, 55128 Mainz, Germany.
[2]Geophysics Department, Tel Aviv University, Tel Aviv, Israel

Correspondence: Volkmar Wirth (vwirth@uni-mainz.de)

Abstract. Resonant amplification of Rossby waves along a circumglobal jetstream was recently hypothesized as the underlying mechanism for the occurrence of extreme weather in observed episodes with large wave amplitudes. An important part of the argument is based on refractive index theory in the framework of the linear barotropic model. The approach makes a number of assumptions and approximations with the goal to diagnose the existence of a zonal waveguide and, hence, the potential for Rossby wave resonance. The current paper compares this approach with a recently developed direct numerical method that makes no further assumptions given the chosen framework and is, hence, considered as more trustworthy. The comparison indicates that the occurrence of waveguides as diagnosed from the refractive index method is both qualitatively and quantitatively inconsistent with the occurrence of resonance in the direct numerical method. It is concluded that the previously-used waveguide diagnostic is not a reliable basis for detecting Rossby wave resonance. The code for the direct numerical method is publicly available to encourage its use in future applications.

1 Introduction

It has long been recognized that Rossby waves in a spherical domain can be subject to linear resonance under specific conditions (Haurwitz, 1940; Charney and Eliassen, 1949). Like in theoretical physics, resonance occurs if the external forcing projects onto a free mode of the system. In the case of Rossby waves, an important pathway towards resonance is provided through the existence of a zonal waveguide in combination with the zonal periodicity of the domain, allowing meridionally trapped free modes that can be further amplified by the forcing (Hoskins and Karoly, 1981). One may thus obtain a steady increase in wave amplitude as time proceeds, possibly leading to very large values.

Rossby wave resonance and related trends in connection with anthropogenic climate change are important topics, because the resulting large wave amplitudes may lead to extreme weather. To the extent that the forcing stems from stationary sources (such as orography), the saturated resonant waves are stationary, too. This increases the possibility of persistent flow anomalies

https://doi.org/10.5194/egusphere-2026-3648
Preprint. Discussion started: 30 June 2026

which, in turn, may add to the severety of weather extremes (Fragkoulidis et al., 2018). In addition, resonance implies a sensitive dependence of wave amplitude on relevant characteristics of the system such as the pattern of the forcing or the background wind speed; as a consequence, even small changes in the system characteristics may be associated with large changes in wave amplitude.

The topic of Rossby wave resonance has attracted renewed interest since the work of Petoukhov et al. (2013) and Kornhuber et al. (2017b), who aimed to explain the occurrence of extreme weather in specific episodes. Key in their analysis was a diagnostic method with the goal to establish resonance as the underlying mechanism for observed large wave amplitudes. Essentially, the authors considered horizontal wave propagation in the framework of the linear barotropic model. A basic tenet in their approach was the idea that the existence of a circumglobal jet waveguide is a necessary precondition for the occurrence of Rossby wave resonance. For the purpose of waveguide detection they used ideas from ray tracing theory pioneered by Hoskins and Karoly (1981). The analysis boils down to computing a "refractive index", which is a function of latitude, and checking whether or not it has a relative maximum in close proximity to the jet. The occurrence of a relative maximum implies the existence of two turning latitudes, where the meridional group velocity would change its sign along the ray path. It follows that the entire wave activity is confined in the region between the two turning latitudes, and one thus obtains a perfect waveguide. The requirement that the refractive index must have two turning latitudes will be referred to as "waveguide criterion" in the remainder of this paper. In combination with a few further criteria the authors finally arrived at their diagnostic for Rossby wave resonance. The resulting method will henceforth be referred to as "(Petoukhov-Kornhuber) refractive index method".

In the following years, the refractive index method was employed by numerous authors in their attempt to prove resonant amplification as the underlying mechanism for the occurrence of large wave amplitude episodes (e.g., Petoukhov et al., 2016; Coumou et al., 2014; Stadtherr et al., 2016; Kornhuber et al., 2017a; Mann et al., 2017, 2018; Kornhuber et al., 2019; He et al., 2023; Guimaraes et al., 2024; Li et al., 2024, 2025). In fact, Rossby wave resonance has become a popular narrative in parts of the scientific community in connection with recent weather extremes. Incidentally, the phenomenon has been referred to by varying terminology, including "quasi-resonance" or "quasi-resonant amplification", short: QRA, (Petoukhov et al., 2013; Coumou et al., 2014; Mann et al., 2018; Guimaraes et al., 2024), "(planetary) wave resonance" (Stadtherr et al., 2016; Kornhuber et al., 2017a, b; Mann et al., 2017; He et al., 2023; Li et al., 2025), or "atmospheric resonance" (Li et al., 2024). Yet, in all quoted papers the diagnostic framework is identical to that of Petoukhov et al. (2013) and Kornhuber et al. (2017b). Here, we choose the term "Rossby wave resonance", because it emphasizes the role of Rossby waves as a key ingredient for the underlying mechanism.

The waveguide criterion of Petoukhov and Kornhuber is based on two levels of assumptions and approximations. First, there is the so-called WKB approximation, which requires that the spatial scale of the wave is much smaller than the scale on which the background state varies. This approximation allows one to use a local dispersion relation for a local Rossby wave solution, thus facilitating analytical progress. However, in the present context the scale of the Rossby waves tends to be larger than the

https://doi.org/10.5194/egusphere-2026-3648
Preprint. Discussion started: 30 June 2026

width of the jet (Wirth, 2020), which renders the WKB approximation suspicious. To be sure, WKB often yields surprisingly realistic results even in situations where the underlying assumptions are barely satisfied, but quantitative discrepancies occur especially in the neighborhood of turning latitudes (Potter et al., 2013), which are important in the present context.

The second level of assumptions completely discounts for the wave nature of the solution and considers, instead, rays along which individual wave packets would travel — the so-called ray tracing technique (Hoskins and Karoly, 1981). On this level, wave activity does not tunnel any longer through forbidden regions (Harnik, 2002). This property presents a serious problem in the present context, because jet waveguides are known to be leaky (Harnik and Wirth, 2025; Wirth and Harnik, 2026), and the ability of a wave packet to tunnel through a forbidden region has a substantual impact on the resulting wave amplitudes. In addition, ray tracing does not account for the global nature of the full solution; this feature does not bode well for the utility of ray tracing either, because the complete meridional structure of the full solution has strong implications for the range of resonant wavenumbers (Wirth and Harnik, 2026).

Given these caveats, it is not surprising that the waveguide criterion has produced results that are in conflict with calculations that do not rely on those underlying assumptions and approximations. For instance, as we have noted above, a jet is generally associated with a finite amount of leakage despite the existence of two turning latitudes, thus invalidating the simple connection between two turning latitudes and a perfect waveguide (Harnik and Wirth, 2025). Also, the waveguide – no waveguide dichotomy was shown to be misleading; rather, waveguidability should be considered as a quantity that varies smoothly between 0 (no waveguide) and 1 (perfect waveguide, cf. Wirth 2020). Furthermore, the waveguide criterion performs poorly in simple model tests (Mooring and Linz, 2026).

It is the goal of the present paper to provide a critical assessment of the refractive index method in general, and the waveguide criterion in particular, as a diagnostic for Rossby wave resonance. Reference for our analysis is the recent work of Wirth and Harnik (2026), who proposed a novel diagnostic for barotropic Rossby wave resonance that does *not* need the above two levels of approximations but, instead, explicitly solves for the meridional wave structure on a given meridional jetstream profile. Broadly speaking, this alternative diagnostic subjects the linearized barotropic vorticity equation to sinusoidal stationary forcing within the jetstream region. A straightforward numerical approach then yields the global wave solution as a function of the zonal wavenumber s. Subsequently, s is varied systematically, and the solution is considered as a function of s. If the amplitude of this solution features a pronounced peak at some intermediate value of s, the jet is considered to support resonance, and the sharpness of the peak can be used to quantify the strength of the resonance. In case of discrepancies between this method and the refractive index method, the former is given priority, because it tests for resonance in a more direct manner and makes less assumptions and approximations. It will henceforth be referred to as the "direct numerical method".

Wirth and Harnik (2026) used Cartesian beta-plane geometry in their analysis. This choice allowed them to compare their numerical solutions for jet-like basic states with analytical solutions for more idealized basic states, thus facilitating the interpretation of their results. In particular they were able to show that the waveguiding property of strong and narrow jets can

https://doi.org/10.5194/egusphere-2026-3648
Preprint. Discussion started: 30 June 2026

be interpreted in terms of partial reflection of wave activity at the periphery of the jet flanks. In the current paper we will, first, adapt their method to spherical geometry; subsequently we consider idealized westerly jets of varying amplitude and width, diagnose their potential for resonance using the direct numerical method, and compare these predictions with those from the waveguide criterion. As we will see, the two approaches can yield conflicting results, indicating serious issues with the refractive index method.

This paper is organized as follows. First, in section 2 we briefly review the physics of resonance and how it applies to Rossby wave dynamics. Subsequently, section 3 describes the barotropic model framework, and section 4 presents the two candidate diagnostics. The main results are contained in section 5, where we compare the predictions from the two methods and elaborate on the use of WKB in combination with matched asymptotics. Finally, section 6 summarizes our results, puts them into perspective, and draws conclusions.

2 The physics of resonance

Resonance is a fundamental concept in theoretical physics arising in connection with the so-called harmonic oscillator (Landau and Lifschitz, 1976). Arguably, one of the simplest physical systems allowing resonance is a point mass attached to a spring. Without external forcing, the point mass may perform an oscillation with frequency ω_0, which is determined by the properties of the system (like the spring constant). In the language of mathematical physics, this free oscillation is referred to as a normal mode, and the frequency ω_0 is called "natural frequency" or "eigenfrequency". If the system is exposed to oscillatory external forcing with frequency ω, i.e., $F'(t) = F_0 \sin\omega t$ with a constant amplitude F_0, the search for a stationary solution yields an oscillation with frequency ω instead of ω_0. The amplitude of this oscillation is given by

$$\mathcal{A}(\omega) = \frac{F_0}{\sqrt{(\omega^2 - \omega_0^2)^2 + \epsilon^2}} \,, \tag{1}$$

where the parameter $\epsilon = \alpha\omega$ (with constant α) represents the effect of damping (Fig. 1a). Apparently, for weak damping the amplitude A depends sensitively on the difference between ω and ω_0, and in the undamped case one obtains a singularity at $\omega = \omega_0$. In addition, the phase difference between the forcing and the response features a discontinuity as one moves across the singularity (no plot shown). Including weak damping regularizes the singularity, but there may still be a pronounced peak in amplitude at $\omega = \omega_0$.

Considering the more general time-dependent problem and starting with an initial condition at rest, resonance in the forced harmonic oscillator materializes as linear growth of amplitude with time. On a deeper mechanistic level, resonance occurs when the temporal structure of the forcing is compatible with the temporal structure of the free oscillation; in this case the forcing is able to continuously transfer energy into the system. In the presence of weak damping, the amplitude eventually saturates at a large value.

https://doi.org/10.5194/egusphere-2026-3648
Preprint. Discussion started: 30 June 2026

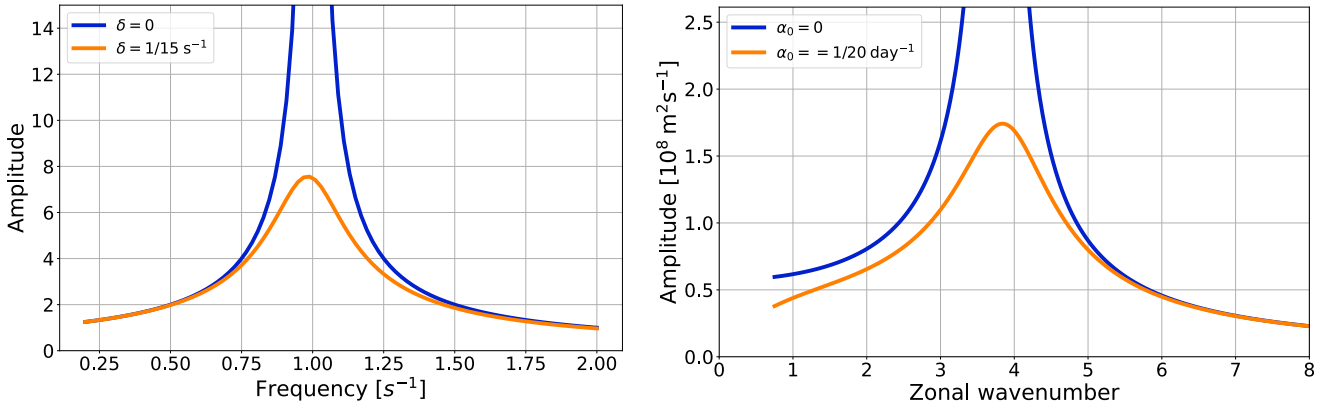

Figure 1. Schematic illustration of the analogy between the forced harmonic oscillator and Rossby wave resonance. (a) Amplitude of the response as function of forcing frequency ω for the classical forced harmonic oscillator. (b) Wave amplitude as a function of the (non-dimensional) zonal wavenumber of the forcing in an idealized model of forced Rossby waves. In both panels, the blue line represents the undamped case, while the orange line represents a case with weak damping.

The above hallmarks of resonance can also be obtained in simple models of Rossby waves excited by external forcing. For instance, consider Rossby waves in the linear barotropic model for a periodic channel with reflecting meridional boundaries and a constant basic state wind U. Let the forcing for the waves be periodic in the zonal direction and go to zero at the boundaries, e.g., $F'(x,y) = kUF_0\cos(ly)\sin(kx)$, where k and l represent the zonal and meridional wavenumber, respectively. The resulting amplitude of the stationary solution can then be written as a function of k as follows:

$$\mathcal{A}(k) = \frac{F_0}{\sqrt{\left[k^2 - (K_s^2 - l^2)\right]^2 + \epsilon^2}}\,. \tag{2}$$

Here, $K_s^2 = \beta/U$ is the square of the stationary wavenumber, β is the meridional gradient of the Coriolis parameter, and the parameter $\epsilon = \alpha(k^2+l^2)/(kU)$ (with constant α) represents the effect of damping. An illustration is given in Fig. 1b. Note the close similarity of the functional dependence for weak or vanishing damping in the expressions (1) and (2), and this is reflected in the similar qualitative behavior of the curves in Figs. 1a and 1b. In addition, one obtains a strong dependence of the phase on the zonal wavenumber (no figure shown). The situation has lucidly been described in the original work of Haurwitz (1940): "The amplitude of a forced perturbation increases as the difference between the wave length of the free perturbation and of the generating force decreases. When the difference vanishes, the amplitude reaches a maximum; resonance occurs. This is analogous to the phenomenon of resonance in the case of harmonic oscillations, except that there the resonance is between the periods of the generating force and of the free oscillation. In the present case where the generating force is a function not of time, but of space, its wave length takes over the role of the period." In other words, resonance occurs when the spatial pattern of the forcing is compatible with the spatial pattern of a free mode, and in this case the forced solution grows linearly with time until the damping (if present) limits the growth.

https://doi.org/10.5194/egusphere-2026-3648
Preprint. Discussion started: 30 June 2026

The basic nature of Rossby wave resonance suggests a straightforward diagnostic method, namely by (i) forcing the system with a meridionally-thin perturbation in the middle of the waveguide (so that it projects onto all meridional normal modes), (ii) systematically varying the zonal wavenumber s of the forcing, and (iii) diagnosing the response as a function of s. Resonance would then be diagnosed whenever the amplitude and the phase of the response depend sensitively on the zonal wavenumber of the forcing — quite like the amplitude and phase of the forced harmonic oscillator depend sensitively on the frequency of the forcing. The above explains the essence of the direct numerical method of Wirth and Harnik (2026).

3 The linear barotropic model framework

In this paper, we consider the barotropic vorticity equation in spherical geometry including external forcing and damping. Linearizing about a zonally symmetric zonal basic state, we obtain

$$\left(\frac{\partial}{\partial t}+\frac{u_0}{a\cos\phi}\frac{\partial}{\partial\lambda}\right)q'+\frac{v'}{a}\frac{dq_0}{d\phi}=-\alpha q'+F'\,. \tag{3}$$

Here, ϕ, λ and t denote latitude, longitude, and time, a is the Earth's radius, $\alpha\geq 0$ is a damping coefficient, F' is the forcing, q' is the perturbation absolute vorticity, and v' is the perturbation meridional wind. Furthermore, $u_0(\phi)$ represents the basic state zonal wind; the latter may depend on latitude, allowing us to represent a midlatitude jet. The meridional gradient of basic state absolute vorticity is given by

$$\frac{1}{a}\frac{dq_0}{d\phi}=\frac{2\Omega}{a}\cos\phi-\frac{1}{a}\frac{d}{d\phi}\left[\frac{1}{a\cos\phi}\frac{d}{d\phi}(u_0\cos\phi)\right]\,, \tag{4}$$

with Ω denoting the Earth's angular rotation. The perturbation absolute vorticity and the perturbation meridional wind can be expressed through the perturbation streamfunction ψ' as

$$q'=\nabla^2\psi' \tag{5}$$

and

$$v'=\frac{1}{a\cos\phi}\frac{\partial\psi'}{\partial\lambda}\,, \tag{6}$$

respectively, where ∇^2 is the horizontal Laplacian operator in spherical coordinates.

The forcing $F'(\lambda,\phi)$ is assumed to be stationary. It is specified in terms of a dimensionless pseudo-orography $h'(\lambda,\phi)$ as

$$F'(\lambda,\phi)=-\frac{f_0u_0}{a\cos\phi}\frac{\partial h'}{\partial\lambda}\,, \tag{7}$$

where $f_0=2\Omega\sin\phi_J$ denotes the Coriolis parameter and ϕ_J is the jet latitude at which u_0 reaches a local maximum (cf. Wirth and Harnik, 2026). In the entire paper we restrict our attention to orography which is sinusoidal in longitude, i.e.,

$$h'(\lambda,\phi)=H(\phi)\,\Re\,e^{is\lambda}\,, \tag{8}$$

https://doi.org/10.5194/egusphere-2026-3648
Preprint. Discussion started: 30 June 2026

where s is the dimensionless zonal wavenumber, $\Re\ldots$ denotes the real part of what comes to the right of it, and the function $H(\phi)$ characterizes the meridional profile of the orography. Note that $H(\phi)$ is independent of s, i.e., we use the same forcing amplitude for all zonal wavenumbers.

As is well known from previous work, the meridional profile of the basic state wind $u_0(\phi)$ has a crucial impact on wave-guidability and, hence, on the resonant behavior (Manola et al., 2013; Wirth, 2020; Wirth and Harnik, 2026). In this paper we use a similar approach as in Wirth (2020) and specify $u_0(\phi)$ as a superposition of westerly solid-body rotation and a westerly Gaussian jet. The four parameters to define the profile are the center latitude ϕ_J of the jet, the strength U_J of the wind at the jet core, i.e., $U_J = u_0(\phi_J)$, the width σ_J of the jet, and the strength $U_{\rm SB}$ of the underlying solid-body rotation at ϕ_J. The details are given in the appendix. Throughout this paper we use $\phi_J = 45°\text{N}$ and $U_{\rm SB} = 5\ \text{m s}^{-1}$, while U_J and σ_J are allowed to vary in order to explore the resulting changes in resonant behavior. In addition, we mostly use $U_J > U_{\rm SB} > 0$ corresponding to a westerly midlatitude jet superimposed on weak westerly solid-body rotation; a pure solid-body rotation basic state can be obtained by setting $U_J = U_{\rm SB}$. Examples for basic state profiles with different values of U_J and σ_J are given in the left column of Fig. 2.

Looking for stationary solutions of the form

$$\psi'(\lambda,\phi) = \Re\,\hat{\psi}_s(\phi)\,e^{is\lambda} \tag{9}$$

reduces (3) to the following ordinary differential equation for the meridional structure function $\hat{\psi}_s(\phi)$,

$$(1-i\tilde{\epsilon})\cos\phi\,\frac{d}{d\phi}\left(\cos\phi\,\frac{d\hat{\psi}_s}{d\phi}\right) + \left[\hat{K}_s^2 - (1-i\tilde{\epsilon})s^2\right]\hat{\psi}_s = -a^2\cos^2\phi\,f_0 H(\phi)\,. \tag{10}$$

Here,

$$\tilde{\epsilon}(\phi) = a\cos\phi\,\frac{\alpha(\phi)}{s\,u_0} \equiv \frac{\alpha(\phi)}{k u_0}\,, \tag{11}$$

with the dimensional zonal wavenumber

$$k = \frac{s}{a\cos\phi}\,. \tag{12}$$

Note that k is a function of latitude for any given value of s. Moreover, the variable

$$\hat{K}_s^2(\phi) = a^2\cos^2\phi\,\frac{1}{u_0}\frac{dq_0}{a\,d\phi} \tag{13}$$

represents the square of the non-dimensional stationary wavenumber. The function $\hat{K}_s(\phi)$ plays a key role in the refractive index method, and it is also an important factor in our equation (10). Note that (10) turns singular at the critical latitudes, i.e., at those latitudes in the interior of the domain where $u_0(\phi) = 0$. However, in our analysis we focus on purely westerly profiles of $u_0(\phi)$ thus avoiding this problem.

https://doi.org/10.5194/egusphere-2026-3648
Preprint. Discussion started: 30 June 2026

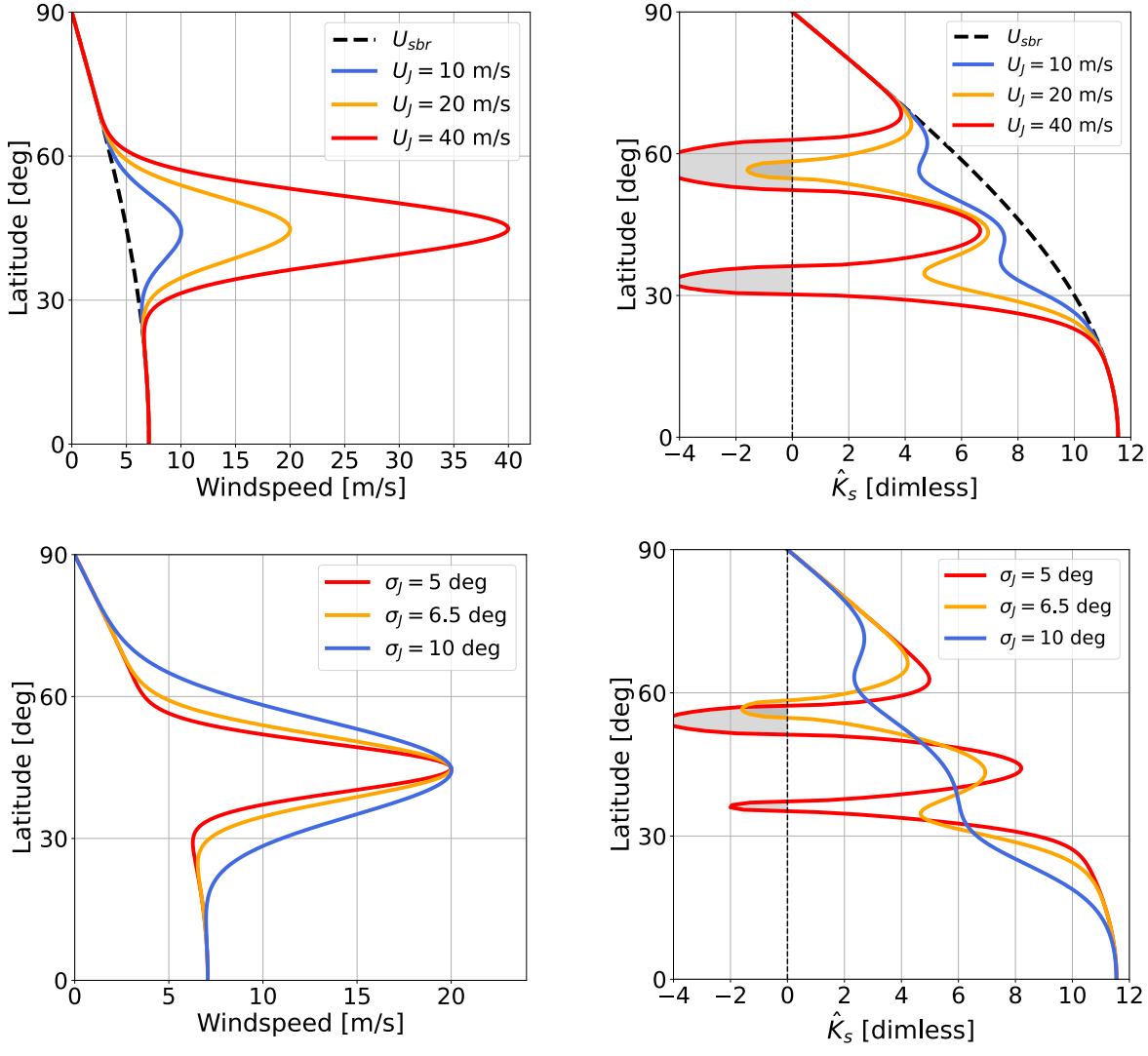

Figure 2. Illustration of different basic states with different jet width and jet strength. The left column shows the wind $u_0(\phi)$, and the right column shows the stationary wavenumber $\hat{K}_s(\phi)$. The top row represents three basic states for three different values of U_J (with $\sigma_J = 6.5°$ held fixed), while the bottom row represents three basic states for three different values of σ_J (with $U_J = 20\ \mathrm{m\,s^{-1}}$ held fixed). The black dashed line in the top row represents the underlying solid-body rotation. The vertical dashed lines in the plots for $\hat{K}_s$ highlight the value 0, and negative values represent minus the imaginary part of $\hat{K}_s$ (gray shading).

https://doi.org/10.5194/egusphere-2026-3648
Preprint. Discussion started: 30 June 2026

4 Two different methods to diagnose Rossby wave resonance

4.1 Refractive index method of Petoukhov and Kornhuber

The gist of the refractive index method is the waveguide criterion, which aims to infer the existence of a waveguide and, hence, the potential for resonance from the profile of $\hat{K}_s(\phi)$, without actually solving any equation. Examples for profiles of $\hat{K}_s(\phi)$ are given in the right column of Fig. 2. Solid-body rotation is associated with a smooth variation $\hat{K}_s(\phi) \propto \cos\phi$. The addition of a midlatitude jet leads to local deviations from this cosine-profile, with an increasingly conspicuous relative maximum at jet latitude as the jet strength increases or the jet width decreases.

Figure 3 explains the argument that connects the profile of $\hat{K}_s(\phi)$ with the potential existence of a waveguide. Given an intermediate zonal wavenumber s, a latitude ϕ_T at which $\hat{K}_s(\phi_T) = s$ may separate the jet region (where $\hat{K}_s(\phi) > s$) from a region outside the jet (where $\hat{K}_s(\phi) < s$). Assuming that the latitudinal variation of the basic state is gradual, the solution can locally be approximated as a plane wave in the jet region, while it is exponential outside the jet region. In the jet region, the dispersion relation allows one to determine a local group velocity. Wave packets can then be assumed to travel along ray paths, i.e., lines that are tangential to the local group velocity. In this framework the points where the character of the solution changes from wavelike to exponential are referred to as "turning points" or "turning latitudes". As is turns out, rays that approach a turning latitude from within the jet region change their meridional direction of propagation and are refracted back towards the jet core (Harnik, 2002). If both equatorward and poleward propagating wave packets within the jet region encounter such a turning latitude, the wave activity is entirely confined to the latitudinal band between the two turning latitudes. This argument suggests that the existence of two turning latitudes for a given wavenumber s signifies a perfect zonal waveguide for that wavenumber, with no leakage across the turning latitudes.

Given that a jet is associated with a relative maximum of $\hat{K}_s(\phi)$ (see Fig. 2), one obtains a range of values for s that are associated with two turning latitudes and, hence, a perfect waveguide, allowing the occurrence of meridionally trapped normal modes. Correspondingly, the waveguide criterion was used as a predictor for the occurrence of resonance. For instance, Fig. 4 in Petoukhov et al. (2013) shows the refractive index from three distinct episodes, two of which indicate a waveguide according the criterion and one does not. As it tuns out, the two waveguide episodes were episodes with extreme weather, while the third episode was not. This was then interpreted as circumstantial evidence that the extreme weather in these two episodes must have been due to resonant amplification of Rossby waves.

The waveguide criterion was combined with further conditions including a threshold on the observed forcing as well as an "amplitude test", where observed wave amplitudes are compared with analytically computed wave amplitudes (see Kornhuber et al., 2017b). These additional criteria involved a number of crude approximations as well as conceptional issues:

https://doi.org/10.5194/egusphere-2026-3648
Preprint. Discussion started: 30 June 2026

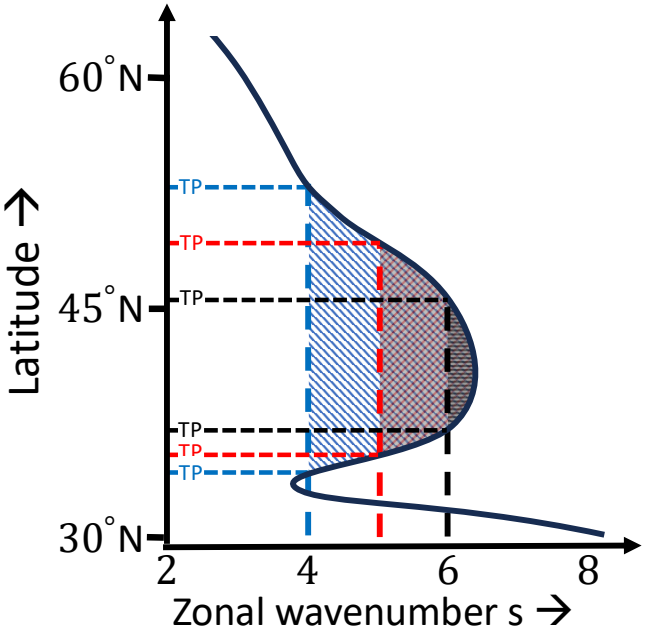

Figure 3. Illustration of the waveguide detection algorithm in the framework of the refractive index method. The solid black line depicts the stationary wavenumber $\hat{K}_s$ as a function of latitude. The different colors represent three zonal wavenumbers s = 4, 5 and 6, and the corresponding 'turning points' are marked as 'TP'. Shading illustrates where waveguides exist for these wavenumbers (figure inspired by White and Admasu 2025).

1. A threshold on the observed forcing does not appear to be a very discriminative criterion. After all, the amplitude of the response is proportional to the strength of the forcing in any linear system, no matter whether the observed (large) response is due to resonance or not. In other words, the hallmark of resonance is not the large size of the numerator on the right hand side of (2), but the small size of the denominator in this expression. Moreover, it is the denominator that leads to the large sensitivity of the response amplitude and phase to small changes in the basic state or the forcing pattern.

2. The expression for the forcing in Petoukhov et al. (2013) and Kornhuber et al. (2017b) includes observed low-frequency temperature anomalies. As a consequence, the forcing threshold implies that episodes with small wave amplitudes are effectively eliminated from being identified as potentially resonant. This device prevents the detection of "false positives", i.e., events in which the diagnostic finds resonance but the observations show small wave amplitudes. The method thus prevents the possibility of straightforward observation-based falsification, which must be considered problematic from an epistemological point of view (Popper, 2004).

https://doi.org/10.5194/egusphere-2026-3648
Preprint. Discussion started: 30 June 2026

3. The analytical formula in the amplitude test assumes, amongst others, that the jet acts as a perfect waveguide. This assumption was later shown to be quantitatively inappropriate (Wirth, 2020; Harnik and Wirth, 2025; Wirth and Harnik, 2026).

For these reasons, we refrain from considering the additional criteria in our main analysis and focus on the waveguide criterion as a predictor for resonance. We will come back to the additional criteria in section 6, where we argue that they do not alter our conclusions.

4.2 Direct numerical method of Wirth and Harnik

The direct numerical method of Wirth and Harnik (2026) considers a model configuration where waves are generated close to the jet core, and any wave activity that leaks out of the jet region is eliminated through sponges. The full wave solution ψ' for this problem is then obtained numerically. The model design focuses attention on the jet waveguide and its propensity to generate resonance.

To specify the forcing, we define the function $H(\phi)$ in (8) as

$$H(\phi) = \begin{cases} \cos\left(\pi \frac{\phi-\phi_J}{\Delta\phi}\right) & , \phi_J - \frac{\Delta\phi}{2} \le \phi \le \phi_J + \frac{\Delta\phi}{2} , \\ 0 & , \text{else} . \end{cases} \tag{14}$$

We choose $\Delta\phi = 8°$, which makes the forcing "meridionally thin" in the sense that its meridional extent is somewhat smaller than typical jet widths considered; at the same time, $\Delta\phi$ is large enough such that it is numerically represented by a fair number of grid points (see below). For illustration, Fig. 4a shows the pseudo-orography for $s = 4$ and $\phi_J = 45°$.

The damping coefficient α is allowed to depend on latitude and specified as a sum of two parts,

$$\alpha(\phi) = \alpha_0 + \alpha_{\mathrm{sp}}(\phi) . \tag{15}$$

Here, $\alpha_0 \ge 0$ is a constant value that is meant to represent the overall effect of damping. In the present paper we only consider the special case $\alpha_0 = 0$, but we included the option of a nonzero value for future use. By contrast, we are going to make essential use of the second part $\alpha_{\mathrm{sp}}(\phi)$, allowing us to design sponges which remove any wave activity that escapes the jet region. While the value of α_{sp} is zero within the jet region, it is positive outside the jet region and increases towards the poles (Fig. 4b). More specifically, there are two sponges, one towards the North Pole and the other one towards the South Pole. Nonzero values of α_{sp} start at $\phi_J \pm 2\sigma_J$, and the strength of the damping in the sponges increases close to exponentially towards the respective poles, where they reach a value of 3 day^{-1}. More details about the sponge design can be found in Harnik and Wirth (2025).

As boundary conditions for (10) we specify $\hat{\psi}(y) = 0$ at both poles, consistent with strong damping in the sponges outside the jet region. Equation (10) plus boundary conditions represents a one-dimensional boundary value problem, which we treat

https://doi.org/10.5194/egusphere-2026-3648
Preprint. Discussion started: 30 June 2026

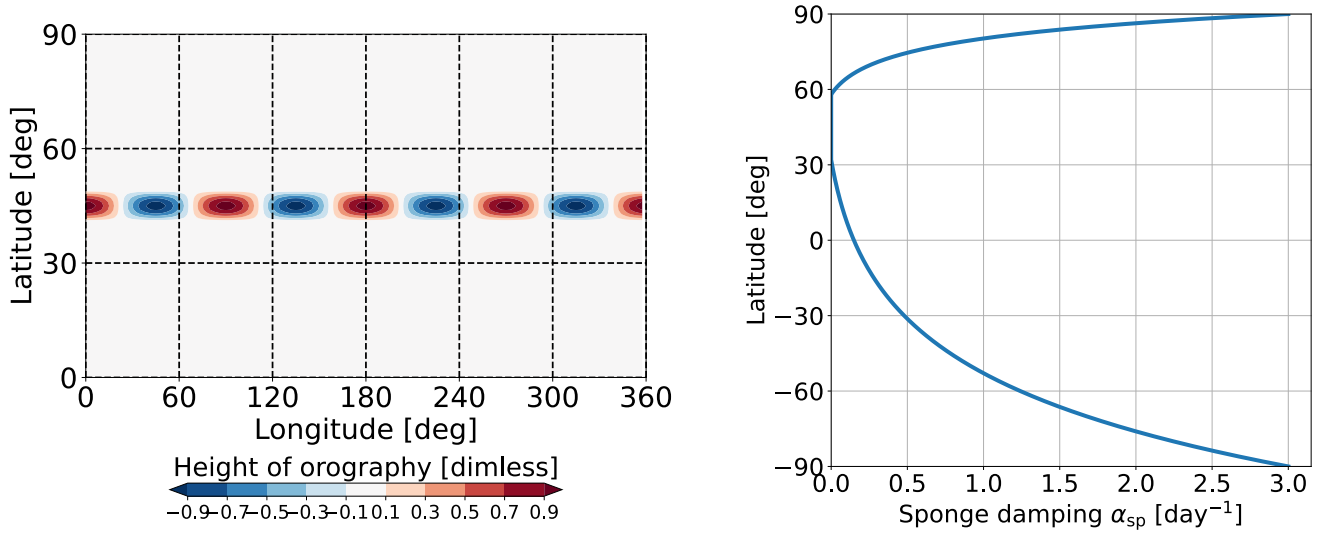

Figure 4. Illustration of the forcing and the sponges used in the direct numerical method. Panel (a) shows pseudo-orgraphy $h'(\lambda, \phi)$ for $s = 4$; panel (b) shows the function $\alpha_{sp}(\phi)$, which represents the damping within the sponges. Both plots are meant to represent a scenario in which the jet is at $\phi_J = 45°$, i.e., the forcing is centered at the jet core and the sponges are outside the jet region.

numerically in a straightforward manner. The differential operator on the left hand side of (10) is discretized using standard finite differences with a resolution of $\delta\phi = 0.5°$ in latitude (unless stated otherwise), reducing the solution for the interior grid points to the inversion of a square matrix. The resulting problem is solved numerically using the linear algebra routine `solve_banded` from `scipy`.

As explained earlier, the diagnostic strategy of Wirth and Harnik (2026) transfers the insight from the harmonic oscillator to the physics of Rossby waves. With our current model configuration this means that we compute solutions ψ' for an entire range of zonal wavenumbers s using the same forcing amplitude $H(\phi)$, and then evaluate how the amplitude and phase of ψ' change as a function of s. The amplitude of the response is defined as

$$A(s) = \max_{\phi} |\hat{\psi}_s(\phi)| \,, \tag{16}$$

where the maximum is determined over the entire range of latitudes between the South Pole and the North Pole. The phase of the response is defined as

$$P(s) = \arctan \frac{\Im\, \hat{\psi}_s(\phi_J)}{\Re\, \hat{\psi}_s(\phi_J)} \,, \tag{17}$$

where $\Im \ldots$ denotes the imaginary part. The basic state is then associated with resonant behavior to the extent that $A(s)$ shows a pronounced peak at one or several values of s, in combination with a pronounced phase shift, i.e., a significant change in $P(s)$ at these wavenumbers. In fact, for the current purpose we can consider s to be a positive real number (rather than an

https://doi.org/10.5194/egusphere-2026-3648
Preprint. Discussion started: 30 June 2026

positive integer), because the meridional structure problem (10) is effectively ignorant of the boundary conditions in the zonal direction and, therefore, well-posed for any real value of s. Obviously, true resonant solutions require s to be an integer; we simply consider real values of s as a simple device to interpolate the functions $A(s)$ and $P(s)$ between those integer values.

Furthermore, we are going to measure the strength of the resonance by using the metric Q from Wirth and Harnik (2026). Assuming that the function $A(s)$ shows one resonant peak only, the metric quantifies the sharpness of this peak. Essentially, we determine the resonant wavenumber s_{res} as the location where the function $A(s)$ maximizes, and we define

$$Q = \frac{2A(s_{\mathrm{res}})}{A(s_{\mathrm{res}}-1)+A(s_{\mathrm{res}}+1)} - 1\,. \tag{18}$$

The metric is designed such that $Q = 0$ if $A(s)$ is a constant function, and Q increases to the extent that the maximum represents an increasingly narrow peak. The value $Q = 1$ is reached when (for a symmetric peak) the maximum value is twice as large as the ambient values at a distance $\Delta s = \pm 1$. A singularity at s_{res} indicating true resonance would be associated with $Q \to \infty$.

4.3 Key differences between the two diagnostics

We briefly summarize key differences between the two diagnostics methods.

1. The refractive index method discounts the global nature of the solution. Rather, it uses the concept of local ray paths, which requires a number of assumptions and approximations and which cannot represent phenomena like tunneling and leakage. By contrast, the direct numerical method examines global solutions in response to sources and sinks of wave activity and does not require any of the assumptions inherent in ray tracing.

2. The refractive index method is somewhat indirect: it really makes a statement about waveguidability, and the latter is then used (sometimes in combination with other criteria) to infer resonant behavior. By contrast, the direct numerical method tests for resonance in a more direct way by exploiting the hallmark of this phenomenon, namely the sensitive dependence of the response to the zonal wavenumber of the forcing.

3. The direct numerical method allows one to quantify the strength of the resonance, while the refractive index method only makes a binary (yes/no) statement about resonance.

4. The refractive index method allows one to diagnose resonance for a given wavenumber s from the knowledge of the basic state alone. By contrast, the direct numerical method requires a set of full wave solutions for a range of wavenumbers and estimates the potential for resonance based on this set of solutions. At first sight, this makes the direct numerical method look less attractive. However, computing the wave solution just requires the inversion of a one-dimensional boundary value problem, and this can be done at negligible computational cost.

https://doi.org/10.5194/egusphere-2026-3648
Preprint. Discussion started: 30 June 2026

For the reasons in items 1 and 2, the Wirth-Harnik method is considered as the more trustworthy one whenever the two methods yield different results. In fact, given the specific model configuration that we use here, we consider our direct numerical method as benchmark against which the refractive index method can be evaluated.

5 Results

5.1 Direct numerical method of Wirth and Harnik

We start by diagnosing resonant behavior using our direct numerical method. For this purpose, we vary either the jet strength U_J while keeping σ_J constant, or we vary the jet width σ_J while keeping U_J constant (cf. Fig. 2). The results are presented in Figs. 5 and 6. Apparently, variation of jet strength leads to considerable changes in the corresponding amplitude function $A(s)$ concerning both the location and the sharpness of the resonant peak. The peak in Fig. 5a shifts to smaller values of s as U_J is increased; this behavior is consistent with the behavior in the case of a constant basic state wind in a reflecting channel (e.g., equation (32) in Wirth and Harnik, 2026). In addition, the sharpness of the resonant peak increases as jet strength increases (blue to orange to red), while it vanishes almost completely for pure solid-body rotation (black dashed line). These systematic differences in peak location and sharpness are mirrored by related differences in phase behavior (Fig. 6a), with a sharper peak corresponding to a stronger change in phase as one moves across the resonance. The corresponding set of experiments with varying jet width σ_J (Fig. 5b and 6b) yields similar behavior in the sense that a sharper resonant peak in the function $A(s)$ is reflected in a somewhat stronger phase variation $P(s)$ as one moves across the resonance.

Both sets of experiments are consistent with the conventional wisdom about the waveguiding properties of jets: strong and narrow jets are better waveguides than weak and wide jets (Manola et al., 2013; Wirth, 2020), implying that strong and narrow jets must be associated with more pronounced resonance than weak and wide jets. At the same time, the plots do not indicate a true singularity at the resonant wavenumber despite the fact that we did not use any damping in the jet region. As detailed in Harnik and Wirth (2025), this phenomenon is due to the leakage of wave activity in the meridional direction, which is not accounted for in the refractive index method (see also Wirth, 2020). Leakage in this context is similar to damping, and the curves in Figs. 5 and 6 are, indeed, reminiscent of damped resonance.

Figure 7 shows the pattern of the perturbation streamfunction $\psi'(\lambda, \phi)$ at the resonant wavenumber s_{res} for one particular case, namely $U_J = 20\,\mathrm{m\,s^{-1}}$ and $\sigma_J = 6.5°$ (for which $s_{\mathrm{res}} = 4.5$). The maxima and minima in this plot are located at $\phi \approx 45\,°\mathrm{N}$, corresponding to the latitude of the jet core as well as the forcing. Towards the North Pole, ψ' decays with no pronounced phase tilt. This feature is consistent with the fact that $\hat{K}_s(\phi) < s_{\mathrm{res}}$ at these latitudes (see orange line in Fig. 2b), which implies evanescent behavior and, hence, full reflection from the turning latitude. By contrast, towards the equator, the maxima and minima of ψ' have a clear south-west north-east phase tilt, suggesting equatorward wave propagation; the wave

https://doi.org/10.5194/egusphere-2026-3648
Preprint. Discussion started: 30 June 2026

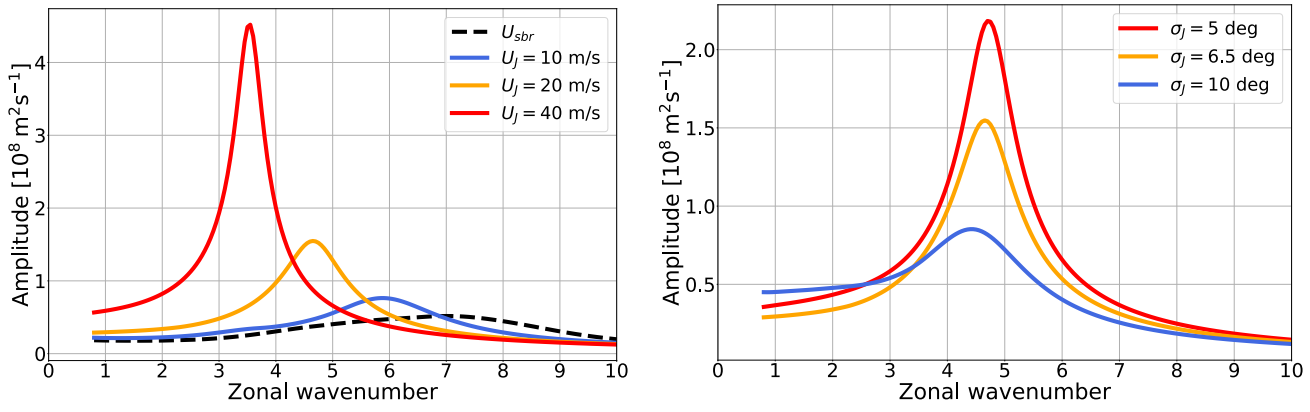

Figure 5. Numerical analysis for different basic states obtained through (a) varying jet strength U_J with constant $\sigma_J = 6.5°$, and (b) varying jet width σ_J with constant $U_J = 20\,\mathrm{m\,s^{-1}}$. The plots show the function $A(s)$, i.e., the amplitude of the response as a function of zonal wavenumber. The different colors refer to different values of U_j or σ_J, respectively, matching the colors in Fig 2. The black dashed line in (a) represents pure solid-body rotation with $U_J = U_{\mathrm{SB}} = 5\,\mathrm{m\,s^{-1}}$.

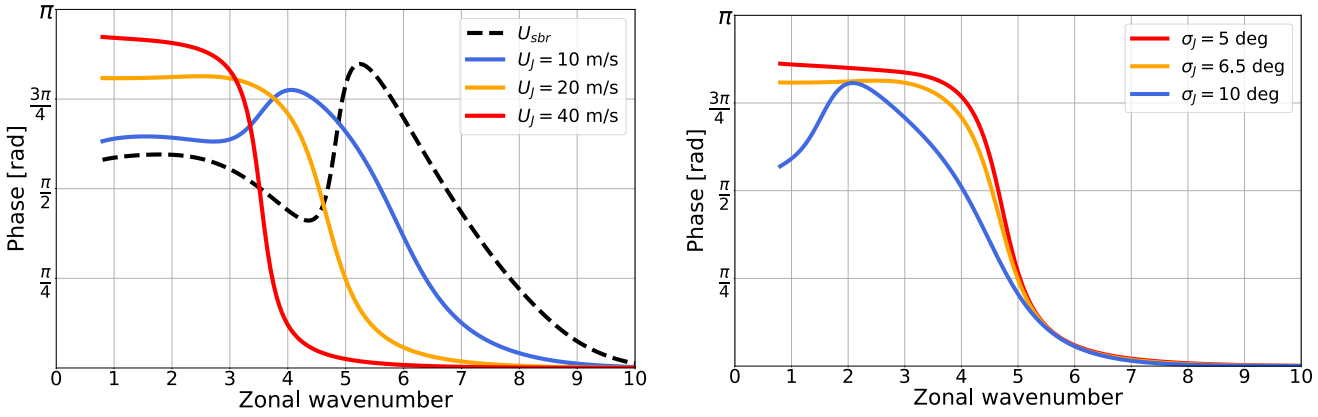

Figure 6. Numerical analysis for different basic states like in Fig. 5, except that the plots show the function $P(s)$, i.e., the phase of the response as a function of zonal wavenumber.

amplitude decreases towards the southern hemisphere due to the damping within the sponge. Physically, the entire pattern can be interpreted as a quasi-mode resembling the first meridional mode, but being modified by leakage towards the tropics (cf. Harnik and Wirth, 2025). The patterns of ψ' for the other combinations of U_J and σ_J from Figs. 5 and 6 look qualitatively similar to the one shown in Fig. 7.

330 Interestingly, in our spherical model version there is no analogue to the pronounced resonant peak for the zero'th meridional mode that we obtained for Cartesian geometry in Wirth and Harnik (2026). As discussed in more detail in that paper, this

https://doi.org/10.5194/egusphere-2026-3648
Preprint. Discussion started: 30 June 2026

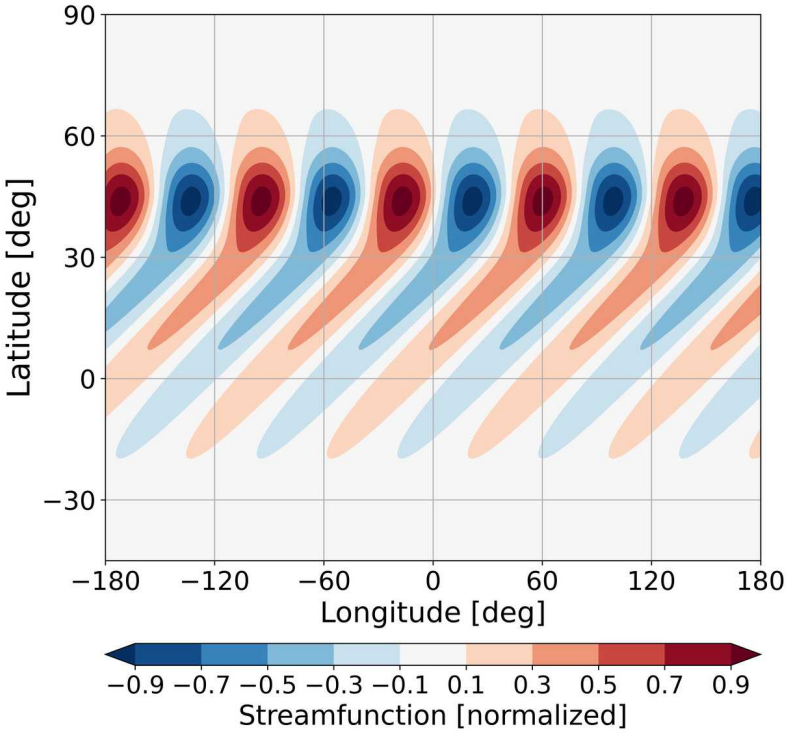

Figure 7. Normalized perturbation streamfunction at $s = s_{\mathrm{res}}$ for $U_J = 20\,\mathrm{m\,s^{-1}}$ and $\sigma_J = 6.5°$ (corresponding to the orange lines in Figs. 5 and 6).

particular mode should be considered an artefact associated with the perfect north-south symmetry for a constant basic state wind in Cartesian geometry. This symmetry has no counterpart in spherical geometry, where ray paths on a solid-body rotation basic state are oriented along great circles (Hoskins and Karoly, 1981). The latter property breaks the north-south symmetry and introduces a preference for equatorward wave propagation. As a consequence, zonal wave ducting through a purely zonal group velocity — being a possibility in Cartesian geometry — cannot be achieved in spherical geometry, and this precludes the resonant peak for the zeroth's meridional mode. Correspondingly, the basic state with solid-body rotation (dashed line in Fig. 5a) does not show any indication of a very sharp peak that could be the analog to what we found in Wirth and Harnik (2026) for a constant basic state.

5.2 Comparison with predictions from the waveguide criterion

We now compare the direct numerical results from the previous subsection with the predictions from the waveguide criterion. Revisiting the right column of Fig. 2, it is easy to check for the occurrence of two turning latitudes for the different basic states. Apparently, in the cases of the weak jet and the wide jet (blue lines in Fig. 2) there is only one turning latitude for any integer s;

https://doi.org/10.5194/egusphere-2026-3648
Preprint. Discussion started: 30 June 2026

hence, the theory predicts "no resonance". This is broadly consistent with our numerical solutions from Fig. 5: although both blue curves in this figure indicate a relative maximum, these maxima are considerably weaker than in the case of the stronger or narrower jets.

Turning to the intermediate case in Fig. 2 corresponding to the orange lines, we see that there are basically two zonal wavenumbers associated with two turning latitudes, namely $s = 5$ and $s = 6$. Possibly, the higher of the two would have been excluded by previous authors owing to an additional criterion that requires a minimum latitudinal spacing between the turning latitudes (Kornhuber et al., 2017b). Accepting this additional rule, the waveguide criterion thus predicts one resonant wavenumber, namely $s = 5$. Indeed, this prediction seems to be in agreement with our numerical results in Fig. 5 (orange lines), which indicate one single peak in both panels; moreover, restricting attention to integer values of s, the largest amplitude of the orange curves in that figure corresponds to $s = 5$.

Finally, we consider the strong and the narrow jet corresponding to the red lines in Fig. 2. In both cases, there are two turning latitudes for all (integer) wavenumbers between 1 and $s_{\max}$ (with $s_{\max} = 6$ in panel b, and $s_{\max} = 8$ in panel d), suggesting an entire range of "resonant wavenumbers". Taken at face value, this would mean that the red curves in Fig. 5 could potentially feature a fair number of individual peaks, one at each integer value $s = 1, 2, \ldots, s_{\max}$. This prediction of multiple resonant wavenumbers is in stark contrast to our direct numerical analysis that predicts only one resonant peak for all considered cases. Indeed, the existence of no more than one resonant peak for realistic jet dimensions was explained in Wirth and Harnik (2026) as a consequence of the strong anisotropy of a jet, i.e., the large difference between its zonal and its meridional scale. Broadly speaking, this anisotropy implies that the first (or "gravest") meridional mode is the only one that can possibly participate in resonance.

We provide yet another example that sheds serious doubt on the reliability of the refractive index diagnostic. For this purpose we consider two jets that have the same strength but slightly different values for the width (Fig. 8a). The corresponding behavior of $A(s)$ in Fig. 8c is qualitatively quite similar for the two jets; in particular, the resonant peaks are almost at the same wavenumber, while the Q-value is 64% larger for the narrower jet. The latter result is consistent with previous findings indicating that narrower jets are better waveguides, in combination with the reasonable expectation that better waveguides are associated with stronger resonance.

Turing to the predictions from the waveguide criterion, we consider the latitudinal profiles of the stationary wavenumber in Fig. 8b. As one can see, the two jets were designed such that the narrower jet is associated with two turning latitudes for $s = 5$, while the wider jet has only one turning latitude for any integer wavenumber within the latitude range of the jet. It follows that the waveguide criterion suggestes the occurrence of resonance at wavenumber $s_{\mathrm{res}} = 5$ for the narrow jet, while it predicts no resonance at any wavenumber for the wider jet. However, this binary contrast between "resonance" versus "no resonance" is not reflected in our direct numerical method illustrated in Fig. 8c: as we saw, our method shows a similar functional dependence of $A(s)$ with a resonant peak in both cases. What is more, the resonant peak in Fig. 8c is very close to $s = 4$ such that the

https://doi.org/10.5194/egusphere-2026-3648
Preprint. Discussion started: 30 June 2026

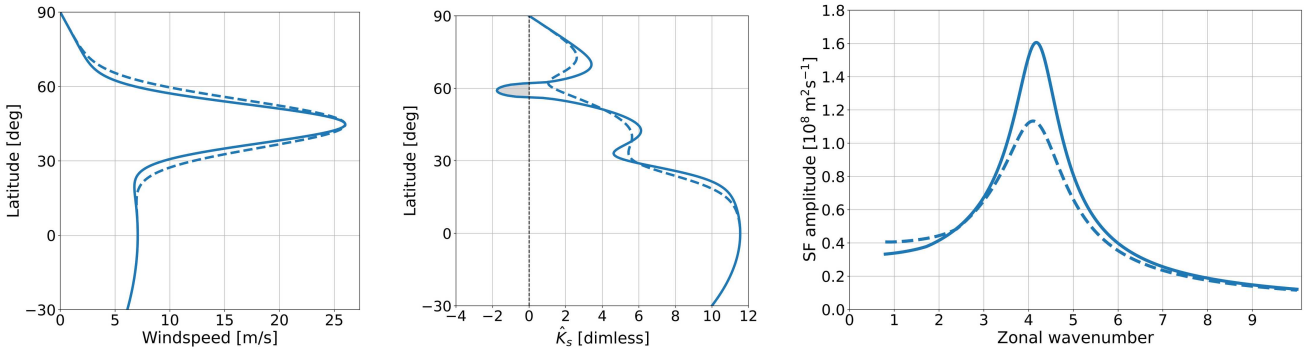

Figure 8. Numerical analysis for two slightly different Gaussian jets. Both jets have $U_J = 26\,\mathrm{m\,s^{-1}}$, but they differ in their width, with the solid line representing $\sigma_J = 7.8^\circ$ and the dashed line representing $\sigma_J = 9.5^\circ$. (a) Meridional profiles of the basic state zonal wind, (b) meridional profiles of the stationary wavenumber $\hat{K}_s$, (c) perturbation streamfunction amplitude $A(s)$. For the resonant peaks in panel (c) we obtained $Q = 1.21$ in case of the narrow jet and $Q = 0.74$ in case of the wider jet. The plot conventions are like in Fig. 2 and 5, respectively.

restriction to integer s would yield $s_{\mathrm{res}} = 4$. Apparently this is in conflict with the waveguide criterion, which would have definitely excluded $s = 4$ from resonance. Thus, our direct numerical method falsifies both the qualitative and the quantitative predictions from the refractive index method in this specific example.

5.3 More systematic analysis

We now generalize the above results by more systematically exploring the jet parameter space. For this purpose we condense the information from the amplitude function $A(s)$ into a single number using the metric Q introduced in (18). This allows us to quantify the strength of the resonance more systematically as a function of jet strength and width. The result is shown in Fig. 9. Apparently, for a given width σ_J, the value of Q increases monotonically with strength U_J (Fig. 9a). Again, this behavior is consistent with the earlier result that stronger jets are better waveguides with less leakage (Manola et al., 2013; Wirth, 2020; Harnik and Wirth, 2025) thus fostering stronger resonance. Both waveguidability and the strength of the resonance show a gradual monotonic dependence on jet strength.

By contrast, the result for varying σ_J with fixed U_J in Fig. 9b indicates a non-monotonic (yet continuous) behavior with a relative maximum at intermediate values of σ_J. The decrease of Q in the limit of small σ_J seems to be in conflict with the general wisdom that narrower jets are stronger waveguides (Manola et al., 2013; Wirth, 2020). However, the range of values for σ_J in these papers was restricted to values larger than about 5°, so there is *a priori* no inconsistency with the current results. At the same time, the asymptotic behavior for small values of σ_J is actually to be expected in light of the effective geometric constraint associated with the meridional quantization (Wirth and Harnik, 2026).

https://doi.org/10.5194/egusphere-2026-3648
Preprint. Discussion started: 30 June 2026

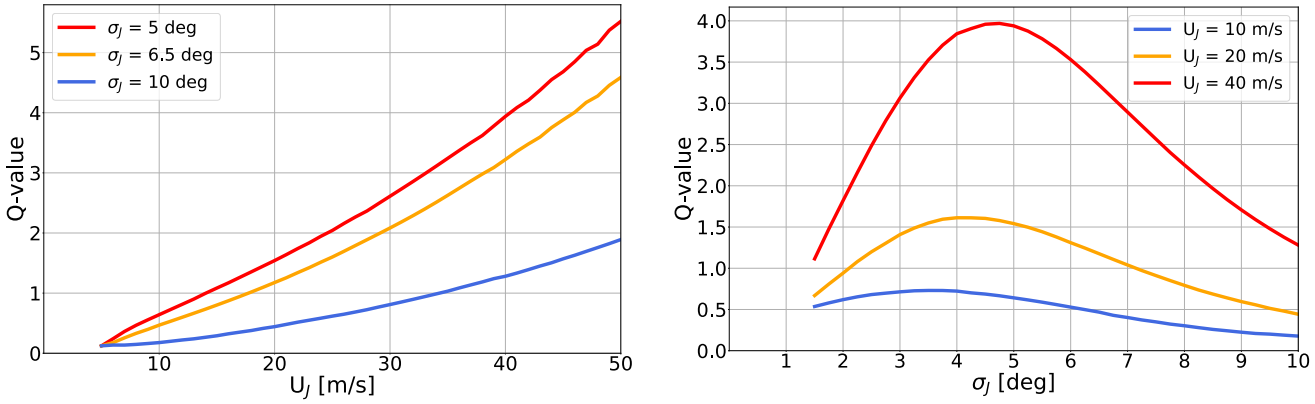

Figure 9. Strength of resonance as quantified by the value of Q from (18), (a) as a function of jet strength U_J (for three different values of σ_J), and (b) as a function of jet width σ_J (for three different values of U_J). The plots were generated by computing the values of Q with a resolution of $\Delta U_J = 1\,\mathrm{m\,s^{-1}}$ in (a), and $\Delta\sigma_J = 0.25°$ in (b); for all computations involving $\sigma_J < 4°$, the meridional grid spacing for solving (10) was refined to $\delta\phi = 0.25°$.

How about the predictions from the waveguide criterion? As mentioned earlier, this criterion only makes a binary decision of whether or not there is resonance. Figure 10 is an attempt to represent this binary decision in our parameter space. Resonance is diagnosed in this plot if the jet is accompanied by a relative maximum of $\hat{K}_s(\phi)$ and if the "depth" of this relative maximum is ≥ 1; this criterion guarantees that there is at least one integer zonal wavenumber with two turning latitudes. Regarding the variation of the jet strength U_J, both metrics — broadly speaking — indicate a more pronounced tendency towards resonance for stronger jets (Fig. 9a and 10a). However, while our metric Q increases gradually for increasing U_J, the waveguide criterion only provides two values corresponding to the existence or the non-existence of resonance. This qualitative difference was already pointed out by Wirth (2020) in the context of waveguidability. The differences are even more striking as one varies the jet width σ_J (Fig. 9b and 10b). On the one hand, our metric Q indicates a maximum in resonant strength at some intermediate value of σ_J, with *decreasing* values of Q in the limit $\sigma_J \to 0$ (as discussed above). On the other hand, the waveguide criterion suggests the occurrence of resonance even for the smallest values of σ_J considered, and the curves in Fig. 10b miss the existence of a relative maximum of our metric Q in Fig. 9b.

More recently, the diagnostic arsenal of the refractive index method has been extended by White and Admasu (2025), in order to account for the fact that the notion of a waveguide as either existent or non-existent is misleading; rather, a waveguide may be stronger or weaker depending on the properties of the basic state. For this purpose, the authors defined the "waveguide strength" for a specific wavenumber s as $w_s = \max(\hat{K}_s - s)$, where the maximum is taken over the latitudinal range between the two turning latitudes (see Fig. 3). Here, we adopt the idea of waveguide strength, but at the same time generalize the concept to make it independent of a specific wavenumber. In the end, we use

$$N_r = \hat{K}_s^{\max} - \hat{K}_s^{\min}\,, \tag{19}$$

https://doi.org/10.5194/egusphere-2026-3648
Preprint. Discussion started: 30 June 2026

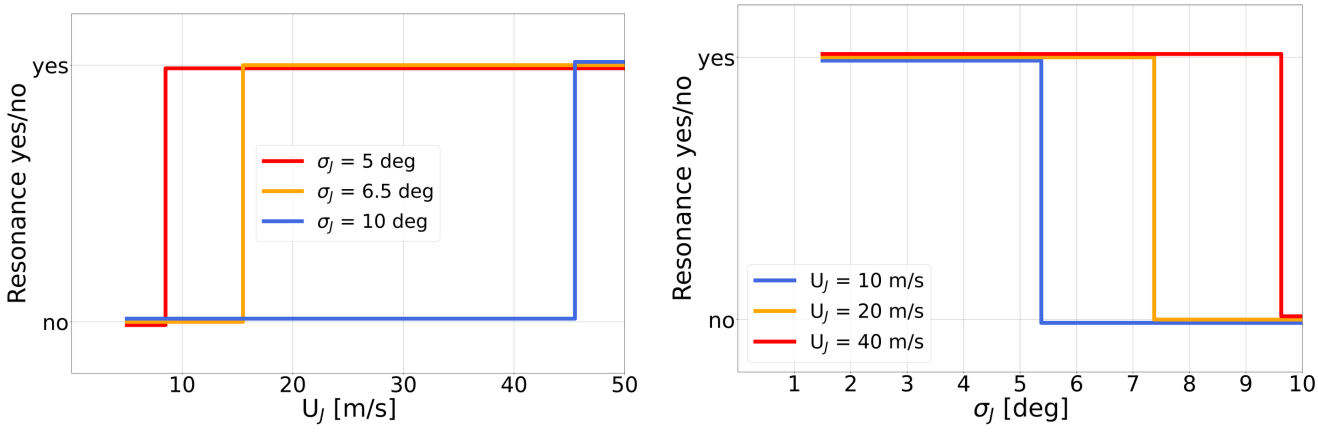

Figure 10. Estimating the occurrence of resonance in the framework of the refractive index method by checking for the existence of two turning latitudes for a least one integer zonal wavenumber (see text). In both plots, the ordinate indicates the presence of absence of resonance. The results are shown in panel (a) as a function of jet strength U_J, and in panel (b) as a function of jet width σ_J. The plots were generated by doing the analysis with a resolution of $\Delta U_J = 1\,\mathrm{m\,s^{-1}}$ in (a), and $\Delta\sigma_J = 0.25^\circ$ in (b). For all computations involving $\sigma_J < 4^\circ$, the meridional grid spacing was refined to $\delta\phi = 0.25^\circ$.

where $\hat{K}_s^{\max}$ denotes the value of $\hat{K}_s(\phi)$ at the relative maximum close to the jet latitude, and $\hat{K}_s^{\min}$ denotes the the value of $\hat{K}_s(\phi)$ at the equatorward relative minimum of $\Re\,\hat{K}_s(\phi)$ if it exists (see Fig. 3). If $\hat{K}_s(\phi)$ increases monotonically towards the equator south of the jet core, we set $N_r = 0$; if, on the other hand, $\hat{K}_s(\phi)$ descends to zero south of the jet core and becomes imaginary at some point, we set $N_r = \hat{K}_s^{\max}$. Broadly speaking, N_r measures the maximum value of w_s over all resonant wavenumbers in the waveguide or, equivalently, the number of values of s that are associated with two turning latitudes. Our metric N_r acknowledges the fact that real wave packets are usually composed of an entire range of zonal wavenumbers. Hence, it appears reasonable to assume that the quality of the waveguide and, therefore, the strength of the resonance is related to the number of wavenumbers for which the basic state serves as a waveguide.

The resulting dependencies of N_r on jet strength and jet width is shown in Fig. 11. By design, the curves now represent continuous functions of the respective abscissa, in contrast with the discontinuous behavior of the curves in Fig. 10. At the same time, comparison with Fig. 9 indicates that there are still striking qualitative differences between the predictions from the waveguide criterion and our metric Q. The most striking difference is the behavior of the curves in panels b in the limit of small σ_J: our metric Q *decreases* for $\sigma_J \to 0$ (Fig. 9b), while N_r keeps *increasing* in that limit (Fig. 11b). The latter behavior can be understood through a simple asymptotic analysis showing that close to the jet core the refractive index behaves as

$$\hat{K}_s(\phi_J) \sim -\frac{1}{u_0}\frac{\partial^2 u_0}{\partial\phi^2}\bigg|_{\phi_J} \sim +\frac{1}{\sigma_J^2} \quad \text{for} \quad \sigma_J \to 0\,, \tag{20}$$

suggesting that N_r must increase for decreasing σ_J. However, as argued above, we have a reasonable understanding for the asymptotic behavior of Q in terms of meridional quantization such that there is no reason to doubt the reliability of our direct

https://doi.org/10.5194/egusphere-2026-3648
Preprint. Discussion started: 30 June 2026

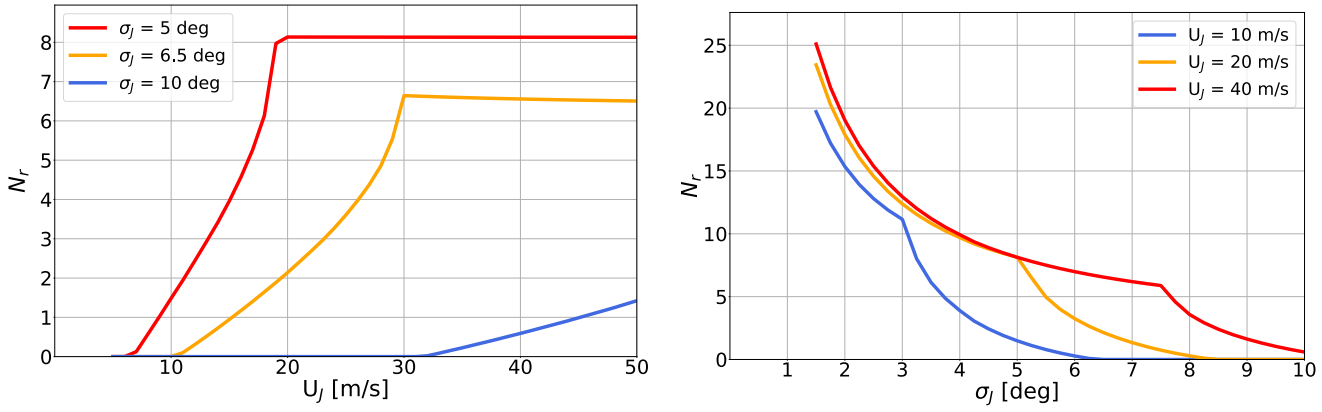

Figure 11. Estimating the strength of resonance in the framework of the refractive index method using the metric N_r as defined in (19). Both plots show N_r, in panel (a) as a function of jet strength U_J, and in panel (b) as a function of jet width σ_J. The plots were generated by computing the value of N_r with a resolution of $\Delta U_J = 1\,\mathrm{m\,s^{-1}}$ in (a), and $\Delta\sigma_J = 0.25°$ in (b). For all computations involving $\sigma_J < 4°$, the meridional grid spacing was refined to $\delta\phi = 0.25°$.

numerical diagnostic. It follows that the number of integer values of s associated with two turning latitudes is not a good measure for the strength of resonance. In other words, the "strength of a waveguide" as foreseen by White and Admasu (2025) is not an indication for its ability to support resonant modes.

5.4 Meridional quantization from WKB theory with matched asymptotics

Earlier we pointed out that the waveguide criterion involves two levels of approximations and assumptions. The second of these, namely ray tracing, reduces attention to the direction of propagation of local wave packets, and this implies that the global-meridional structure of the full solution is not accounted for. Interestingly, the first level of approximations alone, namely the WKB approximation, does allow the construction of global solutions when combined with matched asymptotics. This possibility was mentioned in Petoukhov et al. (2013), but we could not recognize that it is actually used in their analysis. The fact that normal modes are global in nature is important because this leads to quantization behavior with implications for the resonant solutions. In this section we briefly explore the utility of the WKB approximation with matched asymptotics for diagnosing Rossby wave resonance. More specifically, we consider the quantitative differences between the quantization condition in the full numerical solution and that implied by the WKB solution, and how this affects the existence of resonance.

In the absence of forcing and damping, and neglecting the weak variation of $\cos\phi$, our model equation (10) reduces to

$$\frac{d^2\hat{\psi}_s}{d\phi^2} + \left[\hat{K}_s^2(\phi) - s^2\right]\hat{\psi}_s = 0\,. \tag{21}$$

https://doi.org/10.5194/egusphere-2026-3648
Preprint. Discussion started: 30 June 2026

Given a jet profile that is associated with two turning latitudes for a range of zonal wavenumbers as well as purely evanescent behavior outside the jet region, this equation turns into an eigenvalue problem for s. Equation (21) is akin to the stationary Schroedinger equation representing the harmonic oscillator in quantum mechanics. Solutions of this equation in our context are the normal modes which — in the presence of appropriate forcing — would result in resonant behavior. The discrete eigenvalues are associated with the discretization in the meridional direction that was discussed in Wirth and Harnik (2026).

Assuming that the basic state varies gradually, an approximate solution of (21) in the interior of the jet can be obtained using the WKB approximation; this interior solution is subsequently matched to an Airy function in the neighborhood of the two turning latitudes. The condition for this procedure to yield a normal mode solution is

$$\int_{\phi_s}^{\phi_n} \sqrt{\hat{K}_s^2(\phi) - s^2}\; d\phi \;\stackrel{!}{=}\; \left(n - \frac{1}{2}\right)\pi\,, \qquad n = 1, 2, 3, \ldots\,, \tag{22}$$

where n counts the meridional modes, and ϕ_s and ϕ_n denote the southern and northern turning latitude, respectively (Bender and Orszag, 1978). Effectively, this equation represents a constraint for the change of the wave's phase between the two turning latitudes. It can be satisfied only for a discrete set of values $s = s_n$, and this translates to a discrete set of resonant zonal wavenumbers s_{res}.

We put condition (22) to the test for a specific jet. The corresponding profile of $\hat{K}_s(\phi)$ is shown in Fig. 12a; it indicates that this jet is associated with two turning latitudes for any value of s satisfying $2.1 \leq s \leq 6.6$. Within this range, we computed the value of the left hand side of (22) and show the result in Fig. 12b. Apparently, the magnitude of the left hand side in (22) is everywhere smaller than $\pi/2$, which would be the smallest possible value on the right hand side of (22). In other words, WKB theory with matched asymptotics predicts that there cannot be any resonant wavenumber s_{res} for this particular jet. By contrast, our direct numerical solution (not shown) indicates that the jet has one single resonant peak at $s_{\mathrm{res}} = 4.1$ associated with the first meridional mode. For this to be reflected in the WKB solution, the left hand side of (22) would have to be about 50% larger such that the two lines in Fig. 12b intersect at $s = 4.1$. It transpires that a seemingly tolerable quantative deficiency of the WKB approximation results in a complete failure regarding the eigenvalue, i.e., regarding the existence and location of resonance.

We conclude that WKB theory in combination with matched asymptotics is a mixed blessing for our jet-resonance problem. On the one hand, it is able to qualitatively represent the quantization of the meridional modes. This solves the problem pointed out in section 5.2, namely that the existence of two turning latitudes as the only criterion may provide too many "resonant wavenumbers". On the other hand, the foregoing suggests that the approximation is quantitatively deficient to an extent that it must be considered unsuitable for determining the existence and location of the resonant wavenumbers.

https://doi.org/10.5194/egusphere-2026-3648
Preprint. Discussion started: 30 June 2026

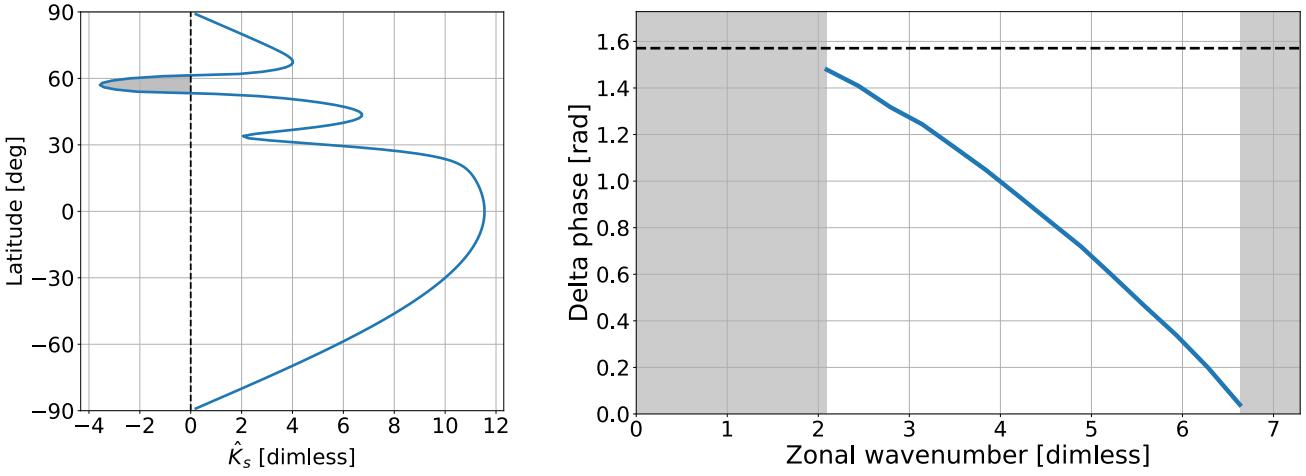

Figure 12. Analysis of the meridional quantization from WKB theory with matched asymptotics for a Gaussian jet with $U_J = 28\,\mathrm{m\,s^{-1}}$ and $\sigma_J = 6.5°$. (a) Latitudinal profile of the stationary wavenumber. (b) Change of phase between the two turning latitudes for the approximate wave solution (solid blue line). The dashed horizontal line denotes the value $\pi/2$, and the grey shading indicates values of s for which the jet is associated with no more than one turning latitude. Resonance associated with the first meridional mode would require that the solid blue line intersects the dashed black line within the non-shaded region.

5.5 Resonance versus jet characteristics

Finally, we use our direct numerical method to quantify the strength of resonance as a function of jet strength and jet width in a single plot (Fig. 13). The plot indicates that — overall — the strength of resonance increases as the jet strength increases and the jet width decreases. However, this general tendency does not hold in the upper right part of the diagram: for strong jets the propensity for resonance with decreasing width reaches a maximum at a specific width, and then decreases for even narrower jets. As detailed in Wirth and Harnik (2026), this behavior can be understood by accounting for the modal structure of resonant solutions in the meridional direction.

6 Summary, discussion, and conclusions

The current paper provides a critical assessment of the refractive index method as a diagnostic for Rossby wave resonance in the framework of the linear barotropic model. For the purpose of benchmark, we extended the direct numerical method of Wirth and Harnik (2026) to spherical geometry, allowing us to diagnose Rossby wave resonance in a more direct manner and with less assumptions and approximations in comparison with the refractive index method. We specified a basic state with an idealized Gaussian jet, and used damping only outside the jet-region in order to design sponges. We then systematically varied

https://doi.org/10.5194/egusphere-2026-3648
Preprint. Discussion started: 30 June 2026

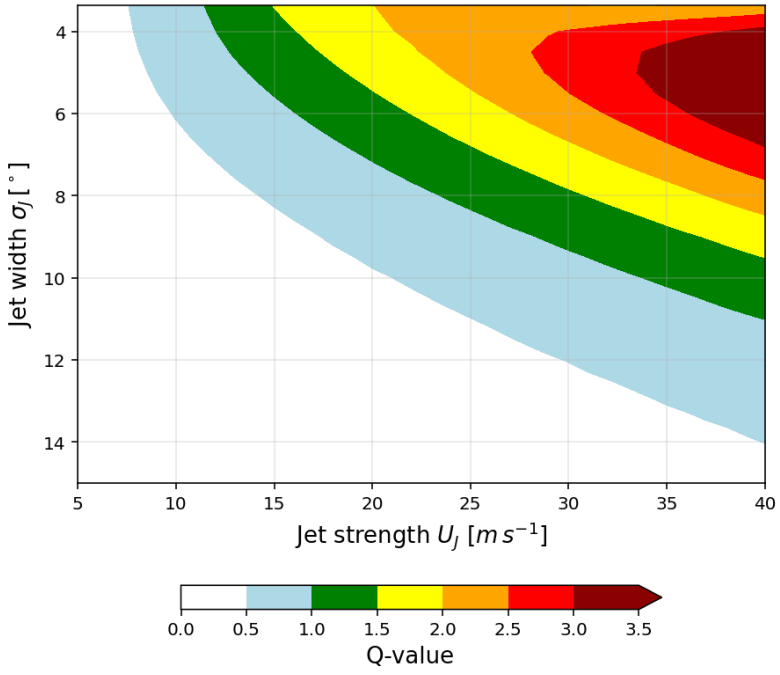

Figure 13. Strength of resonance as measured by the metric Q from the direct numerical method for Gaussian jets as a function of jet strength and jet width. For constructing this plot, the U_J-σ_J-space was discretized by 35 × 24 grid points, and the value of Q was determined for each of these points.

both the strength and the width of the jet and compared the predictions of the waveguide criterion with those from our direct numerical method.

Our main results are the following:

- The strength of resonance (as quantified by our metric Q) changes smoothly as one varies the amplitude or the width of the jet. It follows that the binary concept of resonance as either existent or nonexistent is an oversimplification of the true nature of Rossby wave resonance. This result is consistent with the work of Wirth (2020) who showed that "waveguidability" changes smoothly as the properties of the jet are varied.

- For strong and narrow jets, the waveguide criterion tends to predict a whole range of "resonant wavenumbers" (i.e., wavenumbers associated with two turning latitudes). This prediction is inconsistent with our direct numerical solutions, which featured no more than one resonant peak in all cases considered. The discrepancy can be explained by noting that the search for two turning latitudes as a diagnostic for a perfect waveguide effectively ignores the quantization constraint in the meridional direction associated with the partial reflection near the jet flanks (Wirth and Harnik, 2026).

https://doi.org/10.5194/egusphere-2026-3648
Preprint. Discussion started: 30 June 2026

This deficiency of the waveguide criterion arises from the second level of approximations sketched in the introduction, namely ray tracing, which effectively discounts the global-meridional nature of the solution.

- Even when the waveguide criterion happens to yield exactly one resonant wavenumber s_{res}, the predicted value of s_{res} may be different from the corresponding value from the direct numerical solution. We provided one explicit example for such a discrepancy, and we posit that this single "counter example" is sufficient to shed serious doubt on the trustworthiness of the waveguide criterion for the current application.

- Given a fixed jet strength, the waveguide criterion predicts an *increasing* number of resonant wavenumbers for decreasing jet width. This behavior is inconsistent with our direct numerical solution, which shows only one resonant peak for a narrow jet, and where the sharpness of this peak *decreases* below a certain jet width. The latter behavior is, again, related to the meridional quantization constraint for the reflected part of the solution.

- Given a fixed jet width, the waveguide criterion predicts a sudden saturation of our metric N_r for increasing jet strength. The metric N_r measures the "depth" of a waveguide as deduced from the profile of $\hat{K}_s(\phi)$, and one may be tempted to interpreted it as a predictor for the strength of the resonance. However, this interpretation would be inconsistent with our direct numerical solution, which indicates an ever increasing strength of the resonance as measured by our metric Q. At the same time, our direct numerical solution is consistent with the results of Wirth (2020), which indicate a monotonic increase in waveguidability in this case.

- Interestingly, the first level of approximations alone, namely the WKB approximation, in combination with asymptotic matching allows one to obtain an approximate global solution in the case of two turning latitudes. This technique implies the quantization of the normal modes, which strongly reduces the number of resonant wavenumbers. However, we found that the WKB analysis leads to sizeable discrepancies in comparison with our direct numerical method. This suggests that WKB is not sufficiently accurate for the purpose of diagnosing Rossby wave resonance.

In summary, diagnosing zonal waveguides and, hence, the potential for Rossby wave resonance with the help of the waveguide criterion yields results which are both qualitatively and quantitatively in conflict with our direct numerical method. Considering the latter as benchmark for the chosen model configuration, we conclude that the waveguide criterion cannot be considered as a firm basis for diagnosing resonant behavior.

At this point we come back to the fact that the refractive index method of Petoukhov et al. (2013) and Kornhuber et al. (2017b) involves a number of further criteria, and all criteria are connected through a logical "and". To be honest, the clarity of the description of these further criteria in the quoted papers was occasionally insufficient for our full comprehension. According to our reading, there seems to be a fair number of crude assumptions and approximations being made. However, it is unlikely that the details are very relevant. We are trying to discuss the situation with the help of a schematic (Fig. 14). In this schematic,

https://doi.org/10.5194/egusphere-2026-3648
Preprint. Discussion started: 30 June 2026

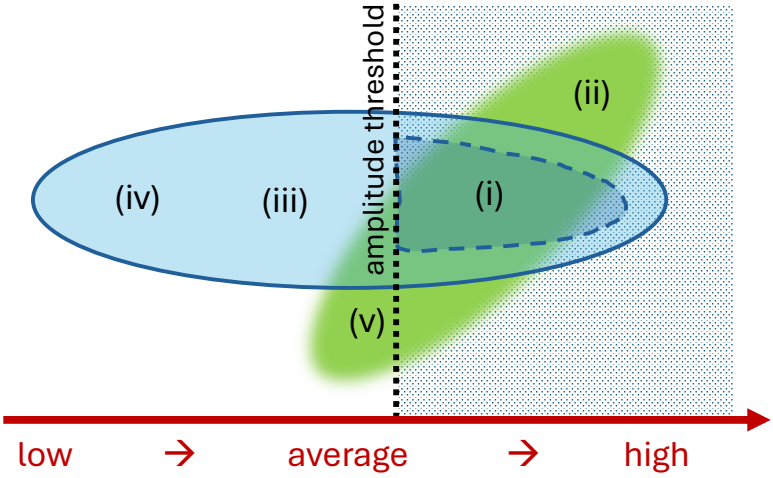

Figure 14. Schematic illustrating the logic behind the refractive index method of Petoukhov and Kornhuber. The two-dimensional plane represents the space spanned by different basic states and different forcings. The green ellipse represents states that are associated with resonance according to our direct numerical method, while the light blue ellipse represents states for which the waveguide criterion diagnoses a perfect waveguide. The red arrows point in the direction is increasing wave amplitudes, and the dotted area to the right of the dotted black line represents above-average wave amplitudes. The symbols (i), (ii) . . . refer to items discussed in the text.

the green ellipse represents the states that are diagnosed as resonant with our direct numerical method,[1] and in the following these states will be referred to as "truly resonant"; at the same time the light blue ellipse represents the states that satisfy the waveguide criterion. The extent to which the two ellipses overlap can be taken as a broad measure of trusworthiness of the refractive index diagnostic.

The analysis in the present paper has shown several properties regarding the geometry of the two ellipses in Fig. 14: (i) the ellipses may overlap, and in this case the joint area of overlap represents states for which the waveguide criterion yields a correct prediction (e.g., $s = 3.5$ in the strong jet case of Fig. 5a, cf. Fig. 2b); (ii) there may be states that are truly resonant but missed by the waveguide criterion (e.g., $s = 4$ in Fig. 8); (iii) there may be states that satisfy the waveguide criterion but that are not truly resonant (e.g., $s = 5$ in the narrow jet case of Fig 8); (iv) the blue ellipse extends well into the region with small wave amplitudes (e.g., $s = 5$ in the strong jet case of Fig. 5a, cf. Fig. 2b). Incidentally, some of the truly resonant states may extend into the region with no more than average wave amplitudes (illustrated as region (v) in Fig. 14), namely when a moderatly strong amount of leakage coincides with weak forcing.

Combining the waveguide criterion with further criteria means that the number of states that are diagnosed as resonant is generally smaller than the number of states that satisfy the waveguide criterion alone. This is illustrated in Fig. 14 by the dashed

[1]Note that we do not advocate resonance as a binary feature, but rather a continuous feature to be measured by a real-valued metric such as our variable Q. For this reason, the green ellipse was drawn with a smooth boundary to indicate the underlying smoothly varying function.

https://doi.org/10.5194/egusphere-2026-3648
Preprint. Discussion started: 30 June 2026

blue semi-ellipse, which (amongst others) accounts for the additional criterion of a forcing threshold. As we have seen, the Petoukhov-Kornhuber forcing threshold corresponds to a threshold on wave amplitude (dotted line in Fig. 14). It may eliminate a fair number of states as being diagnosed resonant and, thus, reduces the problem with the multiple resonant wavenumbers, but other misallocations remain. In fact, we posit that wave amplitude is not a suitable criterion to include in a diagnostic for resonance, because the forcing amplitude acts as a confounder. Rather, it is thet narrowness of the peak as measured by our metric Q that we consider to be the hallmark of resonance, as it diagnoses the properties of the denominator in (2). In any case, the additional criteria can only decrease the area of overlap between the blue and the green regions, and the occurrence of both "false positives" and "missed events" is likely to remain. It transpires that the additional criteria do not necessarily eliminate the mismatch between diagnosed and truly resonant states.

Obviously, the whole idea of analyzing Rossby wave resonance with the help of linear barotropic theory comes with caveats and limitations (for a more comprehensive discussion see Wirth and Harnik, 2026). For once, the barotropic framework discounts the vertical propagation of Rossby waves. However, upward propagation of stationary Rossby waves is restricted to planetary scale waves during the cold season (Charney and Drazin, 1961), which suggests that the barotropic framework may actually be relevant for the questions addressed in the present study (Hoskins and Karoly, 1981; Held et al., 1985). Furthermore, to the extent that nonlinear dynamics start to become relevant, the concept of linear resonance must be considered with care; yet, even then linear theory may still be useful for a qualitative understanding of the general occurrence of large wave amplitudes.

Two more specific caveats of the current work are the following:

- We restricted our analysis to undamped Rossby waves on a circumglobal jet, representing favorable conditions for resonance. In reality, Rossby waves are subject to various forms of damping (in addition to dissipation through jet leakiness), implying that the resonant response may be considerably weaker than documented in our analysis (cf. Harnik and Wirth, 2025). In addition, the resonant behavior may be less pronounced than one might conclude from our analysis to the extent that the jet is not circumglobal.

- We focused on the jet region proper and assumed that any wave activity that leaves the jet region propagates away and is not able to return towards the jet. In other words, we neglected reflection from regions that are located outside the jet region. Yet, the pole or a critical latitude may serve as reflecting surfaces and, thus, affect the resonant behavior (Held, 1983). We are planning to address this issue in our future work. Suffice it to say that our direct numerical method remains well-posed as long as one includes a small amount of damping through a non-zero value of α_0.

Most of these caveats apply to both diagnostic frameworks considered in this paper, and care must be exercised when applying either of them to data from observed episodes. Adding to this, another critical issue is the choice of the wind profile as a basic state in this type of analysis (Wirth and Polster, 2021). However, neither of these issues affects the core of the present

https://doi.org/10.5194/egusphere-2026-3648
Preprint. Discussion started: 30 June 2026

work, which is assessing the utility of the refractive index method for diagnosing Rossby wave resonance within the (limited) framework of the linear barotropic model.

As mentioned before, we consider our direct numerical method to be a better alternative in comparison with the refractive index method. In order to encourage the application of our method, easy-to-use code (namely: `RossbyResonance.py`) was recently published in Hempel and Wirth (2026). On input, the user needs to provide the wind profile $u_0(\phi)$ and the constant damping coefficient α_0; on output the code provides the functions $A(s)$ and $P(s)$ as well as the numbers $s_{\rm res}$ and Q. When applying this code to observed background states, the following questions must be considered:

- Is the jet really circumglobal?
- Is the chosen basic state representative of the jet? Note that in episodes with large-amplitude waves, a combination of zonal and temporal averaging of the zonal wind may not be the best choice (Wirth and Polster, 2021).
- Has an appropriate damping coefficient α_0 been estimated and specified?

Our work implies that diagnosing Rossby wave resonance along a circumglobal jet with the refractive index method comes with serious issues that render it problematic. This conclusion is considered important in the light of numerous previous publications which used this method to diagnose Rossby wave resonance during observed episodes. At the same time, our conclusion is no surprise, because the assumptions and approximations underlying the refractive index method suggest that sigificant deviations from the true wave solution cannot be excluded. To be sure, in practice there may be situations in which the refractive index method happens to provide a correct prediction (corresponding to the intersection between the green and blue ellipse in Fig. 14). But this would have to be considered as fortuitous, and the alleged attribution of resonance as the underlying cause for observed high wave amplitudes remains dubious. Moreover, this study together with the work of Wirth and Harnik (2026) provides a deeper understanding for the failures of the waveguide criterion and, thus, corroborates our conclusions.

The entire state of affairs calls for a careful reevaluation of earlier studies that rely on the refractive index method for diagnosing Rossby wave resonance, like Petoukhov et al. (2013, 2016); Coumou et al. (2014); Stadtherr et al. (2016); Kornhuber et al. (2017a, b); Mann et al. (2017, 2018); Kornhuber et al. (2019); He et al. (2023); Guimaraes et al. (2024); Li et al. (2024, 2025). At this point it is unclear whether their results withstand further scrutiny or not. At the same time, it remains an open question whether or to what extent Rossby wave resonance plays a role in episodes with extreme weather.

Code availability. The code that was used to prepare this paper is available in Hempel and Wirth (2026)

https://doi.org/10.5194/egusphere-2026-3648
Preprint. Discussion started: 30 June 2026

Data availability. This work is based on idealized model simulations which do not use any external data.

Appendix A: Specification of the basic state wind profile

We use the following procedure to specify the basic state profile $u_0(\phi)$:

1. Start with a solid-body rotation profile

$$u_0(\phi) = U_{\mathrm{SB}} \, \frac{\cos\phi}{\cos\phi_J} \, , \tag{A1}$$

   which guarantees that its value equals U_{SB} at jet latitude.

2. Add a Gaussian jet as follows:

$$u_0(\phi) \to u_0(\phi) + (U_J - U_{\mathrm{SB}}) \, e^{-\frac{(\phi-\phi_J)^2}{2\sigma_J^2}} \, . \tag{A2}$$

3. Subtract a linear profile $L(\phi)$ such that the resulting profile satisfies $u_0 = 0$ at the two poles.

4. Multiply the difference between the so-obtained $u_0(\phi)$ and the original solid-body rotation profile with a real number such that $u_0(\phi_J) \stackrel{!}{=} U_J$.

The resulting final profile $u_0(\phi)$ has the desired properties.

Author contributions. V. Wirth conceptualized this work, wrote code, carried through numerical experiments, and took the lead in writing the paper. T. Hempel wrote code, carried through numerical experiments, and contributed to the textual presentation. N. Harnik co-conceptualized this work and made essential contributions in shaping the paper's written content and presentation.

Competing interests. N. Harnik is a member of the editorial board of Weather and Climate Dynamics.

Acknowledgements. The authors gratefully acknowledge helpful comments by M. Riemer on an earlier version of this manuscript. A large language model has been used to improve the formulation of one sentence, otherwise this work is free of artificial intelligence.

https://doi.org/10.5194/egusphere-2026-3648
Preprint. Discussion started: 30 June 2026

References

Bender, C. M. and Orszag, S. A.: Advanced Mathematical Methods for Scientists and Engineers, McGraw-Hill Book Company, 593 pp, 1978.

Charney, J. G. and Drazin, P. G.: Propagation of planetary-scale disturbances from the lower into the upper atmosphere, J. Geophys. Res., 66, 83–109, 1961.

Charney, J. G. and Eliassen, A.: A numerical method for predicting the perturbations of the middle latitude westerlies, Tellus, 1, 38–54, 1949.

Coumou, D., Petoukhov, V., Rahmstorf, S., Petri, S., and Schellnhuber, H. J.: Quasi-resonant circulation regimes and hemispheric synchronization of extreme weather in boreal summer, Proceedings of the National Academy of Sciences, 34, 12 331–12 336, 2014.

Fragkoulidis, G., Wirth, V., Bossmann, P., and Fink, A. H.: Linking Northern Hemisphere temperature extremes to Rossby wave packets, Quart. J. Roy. Met. Soc., 144, 553–566, DOI:10.1002/qj.3228, 2018.

Guimaraes, S. O., Mann, M. E., Rahmstorf, S., Petri, S., Steinman, B. A., Brouillette, D. J., Christiansen, S., and Li, X.: Increased projected changes in quasi-resonant amplification and persistent summer weather extremes in the latest multimodel climate projections, Scientific Reports, 14, https://doi.org/10.1038/s41 598–024–72 787–0, 2024.

Harnik, N.: The Evolution of a Stratospheric Wave Packet, J. Atmos. Sci., 59, 202–217, 2002.

Harnik, N. and Wirth, V.: Quasi-resonance in a leaky waveguide?, J. Atmos. Sci., 82, 1267–1291, https://doi.org/10.1175/JAS–D–24–0031.1, 2025.

Haurwitz, B.: The motion of atmospheric disturbances on the spherical earth, J. Mar. Res., 3, 254–267, 1940.

He, Y., Zhu, X., Sheng, Z., and He, M.: Resonant Waves Play an Important Role in the Increasing Heat Waves in Northern Hemisphere Mid-Latitudes Under Global Warming, Geophys. Res. Lett., p. https://doi. org/10.1029/2023GL104839, 2023.

Held, I., Panetta, R. L., and Pierrehumbert, R. T.: Stationary external Rossby waves in vertical shear, J. Atmos. Sci., 42, 865–883, 1985.

Held, I. M.: Stationary and quasi-stationary eddies in the extratropical troposphere: Theory, in: Large Scale Dynamical Processes, edited by Hoskins, B. J. and Pearce, R. P., pp. 127–168, Academic Press, 1983.

Hempel, T. and Wirth, V.: Python code for a direct numerical method to diagnose barotropic Rossby wave resonance along a circumglobal jetstream, Zenodo. https://doi.org/10.5281/zenodo.18872902, 2026.

Hoskins, B. J. and Karoly, D. J.: The Steady Linear Response of a Spherical Atmosphere to Thermal and Orographic Forcing, J. Atmos. Sci., 38, 1179–1196, 1981.

Kornhuber, K., Petoukhov, V., Karoly, D., Petri, S., Rahmstorf, S., and Coumou, D.: Summertime Planetary Wave Resonance in the Northern and Southern Hemispheres, J. Climate, 30, 6133–6150, 2017a.

Kornhuber, K., Petoukhov, V., Petri, S., Rahmstorf, S., and Coumou, D.: Evidence for wave resonance as a key mechanism for generating high-amplitude quasi-stationary waves in boreal summer, Climate Dynamics, 49, 1961–1979, doi:10.1007/s00 382–016–3399–6, 2017b.

Kornhuber, K., Osprey, S., Coumou, D., Petri, S., Petoukhov, V., Rahmstorf, S., and Gray, L.: Extreme weather events in early Summer 2018 connected by a recurrent hemispheric wave-7 pattern, Environmental Research Letters, 14, 054 002, doi:10.1088/1748–9326/ab13bf, 2019.

Landau, L. D. and Lifschitz, E. M.: Lehrbuch der Theoretischen Physik. Band I: Mechanik, Akademie-Verlag Berlin, 1976.

Li, X., Mann, M., Wehner, M. F., Rahmstorf, S., Petri, S., Christiansen, S., and Carillo, J.: Role of atmospheric resonance and land–atmosphere feedbacks as a precursor to the June 2021 Pacific Northwest Heat Dome event, Proceedings of the National Academy of Sciences, 121, https://doi.org/10.1073/pnas.2315330 121, 2024.

https://doi.org/10.5194/egusphere-2026-3648
Preprint. Discussion started: 30 June 2026

Li, X., Mann, M. E., Wehner, M. F., and Christiansen, S.: Increased frequency of planetary wave resonance events over the past half-century, Proceedings of the National Academy of Sciences, p. https://doi.org/10.1073/pnas.2504482122, 2025.

Mann, M. E., Rahmstorf, S., Kornhuber, K., Steinman, B. A., Miller, S. K., and Coumou, D.: Influence of Anthropogenic Climate Change on Planetary Wave Resonance and Extreme Weather Events, Scientific Reports, 7, 1–10, doi:10.1038/srep45 242, 2017.

Mann, M. E., Rahmstorf, S., Kornhuber, K., Steinman, B. A., Miller, S. K., Petri, S., and Coumou, D.: Projected changes in persistent extreme summer weather events: The role of quasi-resonant amplification, Science Advances, 4, eaat3272, 2018.

Manola, I., Selten, F., de Vries, H., and Hazeleger, W.: "Waveguidability" of idealized jets, J. Geophys. Res., 118, 10,432–10,440, doi:10.1002/jgrd.50 758, 2013.

Mooring, T. A. and Linz, M.: Resonant Rossby wave mechanism for extreme weather performs poorly in simple model test, Sci. Adv., 12, eadp3054, DOI:10.1126/sciadv.adp3054, 2026.

Petoukhov, V., Rahmstorf, S., Petri, S., and Schellnhuber, H.-J.: Quasiresonant amplification of planetary waves and recent Northern Hemisphere weather extremes, Proceedings of the National Academy of Sciences, 110, 5336–5341, doi:10.1073/pnas.1222000 110, 2013.

Petoukhov, V., Petri, S., Rahmstorf, S., Coumou, D., Kornhuber, K., and Schellnhuber, H. J.: Role of quasiresonant planetary wave dynamics in recent boreal spring-to-autumn extreme events, Proceedings of the National Academy of Sciences, 113, 6862–6867, 2016.

Popper, K. R.: Logik der Forschung, Akademie-Verlag, 2004.

Potter, S. F., Spengler, T., and Held, I. M.: Reflection of Barotropic Rossby Waves in Sheared Flow and Validity of the WKB Approximation, J. Atmos. Sci., 70, 2170–2178, 2013.

Stadtherr, L., Coumou, D., Petoukhov, V., Petri, S., and Rahmstorf, S.: Record Balkan floods of 2014 linked to planetary wave resonance, Sci. Adv., 2, e1501 428, 10.1126/sciadv.1501 428, 2016.

White, R. H. and Admasu, L. M.: Temporally and zonally varying atmospheric waveguides — climatologies and connections to quasi-stationary waves, Weather and Climate Dynamics, 6, 549–570, https://doi.org/10.5194/wcd–6–549–2025, 2025.

Wirth, V.: Waveguidability of idealized midlatitude jets and the limitations of ray tracing theory, Weather Clim. Dynam., 1, 111–125, https://doi.org/10.5194/wcd–1–111–2020, 2020.

Wirth, V. and Harnik, N.: Rossby wave resonance for idealized jets on a beta-plane: towards a better understanding of the meridional wave structure, Weather and Climate Dynamics, 7, 297–316, https://doi.org/10.5194/wcd–7–297–2026, 2026.

Wirth, V. and Polster, C.: The problem of diagnosing jet waveguidability in the presence of large-amplitude eddies, J. Atmos. Sci., 78, 3137–3151, https://doi.org/10.1175/JAS–D–20–0292.1, 2021.